

Elastic Building Blocks for Confined Sheets

Robert D. Schroll,¹ Eleni Katifori,² and Benny Davidovitch¹

¹*Physics Department, University of Massachusetts, Amherst Massachusetts 01003, USA*

²*Center for Studies in Physics and Biology, Rockefeller University, New York, New York 10065, USA*

(Received 7 September 2010; revised manuscript received 16 December 2010; published 14 February 2011)

We study the behavior of thin elastic sheets that are bent and strained under a weak, smooth confinement. We show that the emerging shapes exhibit the coexistence of two types of domains. A focused-stress patch is subject to a geometric, piecewise-inextensibility constraint, whereas a diffuse-stress region is characterized by a mechanical constraint—the dominance of a single component of the stress tensor. We discuss the implications of our findings for the analysis of elastic sheets under various types of forcing.

DOI: [10.1103/PhysRevLett.106.074301](https://doi.org/10.1103/PhysRevLett.106.074301)

PACS numbers: 46.32.+x

The geometry and mechanics of elastic sheets have recently become a focus of intense activity [1,2]. This interest has been driven in part by studies that demonstrated its relevance to biological tissues [3,4], and by technological advance that enabled the production of extremely thin films with precise material properties [5,6]. Such thin sheets undergo a buckling instability even under minor compressions, and their typical state is thus far above threshold, where the energetic cost of straining is much larger than that of bending [2]. In such situations traditional perturbation methods for sheets close to buckling threshold [7] are no longer available, and a full nonlinear analysis of the system is required. A major theoretical challenge here is the development of a formalism that effectively addresses the configurations realized by elastic sheets as their thickness becomes exceedingly small. A central question for such a theory is what are the basic “building blocks” that compose these asymptotic shapes.

Singular types of building blocks include developable cones (“*d* cones”) [8,9] and “minimal ridges” [10,11], which are reflected in the branched network of vertices and sharp folds in a crumpled paper [2]. In the limit of an infinitely thin sheet, these asymptote to points or lines. This behavior manifests a consequence of Gauss’s *Theorem Egregium*, according to which patches that are curved in two directions must be strained [2]. These singular structures focus elastic energy in small regions that are highly bent and hence strained, creating an asymptotically *piecewise-inextensible* (origami-like) shape in which the rest of the sheet remains unstrained in flat facets. Stress focusing has been a subject of many studies in the last two decades [2]. However, it has become clear that shapes of thin sheets are not fully describable by the stress-focusing idea. For example, it is known that uniaxial tension leads to smooth wrinkling patterns that are curved (hence strained) everywhere in both directions [12,13]. Even without exerted tension, certain boundary conditions [14] lead to shapes that reflect a smooth distribution of strain and

curvature. It was even proposed that stress focusing may appear only under large confinement [15] or in response to sharp boundaries [11], although recent experiments may suggest otherwise [16]. We are thus led to ask a number of questions: What type of boundary conditions yield singular structures? Are there other basic structures that are necessary for describing the configurations of thin sheets?

Motivated by these questions, we study in this Letter a sheet under simple confinement, representative of the general class of boundary conditions that are not “tailored” to yield a piecewise-inextensible shape. Our results render three important messages: First, we show that a focused-stress structure appears even under weak, smooth confinement. Second, a focused-stress zone may coexist with a large region in which energy is smoothly distributed. This “diffuse-stress” zone constitutes a new, so far largely overlooked, building block. Third, in contrast to stress focusing, diffuse-stress domains are dominated by a mechanical rather than geometrical constraint: a vanishing ratio between compressive and tensile stress components. Our observations suggest a cornerstone for a theory of the asymptotic shapes of thin sheets under general conditions.

Our system, Fig. 1(a), consists of a semi-infinite rectangular sheet of thickness t where one long edge, say $y = W$, is displaced inward by $\tilde{\Delta}W$ with $\tilde{\Delta} \ll 1$. Far from the edge at $x = 0$, a sufficiently thin sheet ($t \ll \sqrt{\tilde{\Delta}}W$) would naturally buckle to an asymptotically x -independent shape $\zeta_1(x, y) = A_1 \cos(\pi y/W)$. At $x = 0$ we impose a “3-buckle” profile $\zeta_3(x = 0, y) = A_3 \cos(3\pi y/W)$, required to lie in the y - z plane. Absence of strain at the boundaries implies: $A_j \approx 2\sqrt{\tilde{\Delta}}W/j\pi$. The transition between the 3-buckle and 1-buckle shapes requires the formation of a strained region, curved in both directions. It is the structure of this strained region that we address here. Our choice of boundary conditions is motivated by several reasons: (a) The strainless 1-buckle and 3-buckle shapes are, respectively, the asymptotic ground state and a low-energy metastable state of the bending

energy (1) under one-dimensional confinement. Similarly to the universal nature of phase transformation, e.g., between solid and supercooled liquid, the transition between these strainless states can be expected to be a generic form for accommodating unavoidable strain, rather than a shape dependent on the specific boundary conditions. In contrast, other studies directly induce strain by pinching [14,17] or flattening [18,19] an edge of a confined sheet. (b) Despite the nontrivial structure of the strained region, the simplicity of our system allows quantitative description both numerically and analytically. This enables us to distinguish between diffuse-stress and focused-stress types of building blocks, and to formulate asymptotic conditions that could be used under more complicated constraints. (c) Beyond the general lessons drawn from this system, it deserves its own right as a “unit cell” of hierarchical, multiscale patterns on elastic sheets [13,18–22].

The configuration of the sheet is found by minimizing the Föppl–von Kármán (FvK) elastic energy, $U = U_S + U_B$, which contains stretching and bending terms [7]:

$$U_S = \frac{1}{2} \int dx dy \sigma_{ij} u_{ij}; \quad U_B = \frac{1}{2} B \int dx dy (\nabla^2 \zeta)^2, \quad (1)$$

$$\sigma_{ij} = \frac{Y}{1-\nu^2} [(1-\nu)u_{ij} + \nu\delta_{ij}u_{kk}]. \quad (2)$$

$Y = Et$ and $B = Et^3/12(1-\nu^2)$ are, respectively, the stretching and bending moduli, E is the Young modulus, and ν is the Poisson ratio. The (geometric) nonlinearity of U comes from the strain $u_{ij} = \frac{1}{2}(\partial_i u_j + \partial_j u_i + \partial_i \zeta \partial_j \zeta)$. We use the software Surface Evolver [23] to minimize U on a rectangular sheet. One end of the sheet is fixed to the 3-buckle shape while the other is free. The sheet is long

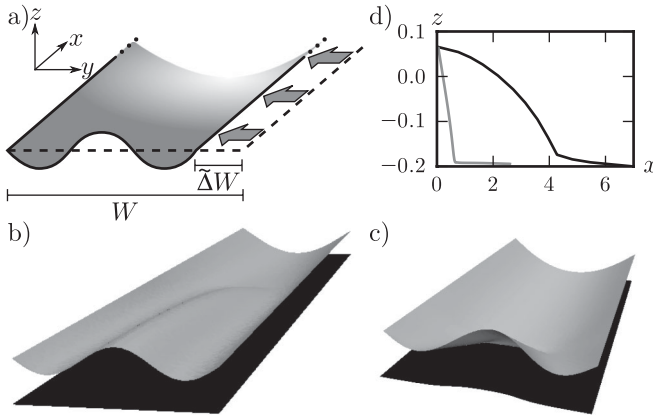


FIG. 1. (a) A semi-infinite sheet of width W confined in one direction by a distance ΔW . The near end is forced into a 3-buckle shape in the y - z plane. (b) The shape of a sheet with $t/W = 0.002$, $\Delta = 0.1$, and $\nu = \frac{1}{3}$. Note the extended smooth area near the prescribed edge, which terminates in a focused structure. (c) When the prescribed edge is allowed to be non-planar, only a focused-stress region emerges. (d) Centerline profiles of the shapes in (b) (black) and (c) (gray).

enough that the free end takes the 1-buckle shape. No bending moment is applied to the long edges.

A representative shape, shown in Fig. 1(b), exhibits two prominent features. First, the transition terminates sharply at a small, stress-focusing zone, beyond which the 1-buckle shape is approached. Notably, this focused-stressed structure appears under weak, smooth confinement, unlike the d cones and ridges of [9–11]. Second, the transition between the two states occurs over a large distance L_t , which diverges as $t^{-1/2}$. Similar scaling was observed in a pinched cylindrical shape [14,24], and was shown to arise from a competition between two dominant energies: excess bending (favoring small L_t) and stretching (favoring large L_t). A similar idea has been noted already in [18–20]. The bending energy is dominated by curvature in the \hat{y} direction, $\kappa \sim \sqrt{\Delta}/W$, while in-plane stretching is dominated by strain along \hat{x} , estimated as $u_{xx} \sim (\frac{\partial \zeta}{\partial x})^2 \sim \Delta(W/L_t)^2$. Balancing these energies $B\kappa^2 \sim Yu_{xx}^2$, we obtain

$$L_t \sim W/\tau^{1/2} \quad \text{and} \quad U \sim EW^3(\tau\Delta)^{5/2}, \quad (3)$$

where $\tau \equiv t/(W\sqrt{\Delta})$ is a (dimensionless) measure of the thickness. Far from buckling threshold $\tau \ll 1$. Notably, this argument suggests that in the transition region stress is not focused; instead stress is smoothly distributed over area WL_t that diverges as $t \rightarrow 0$. Figure 2 demonstrates that the lateral extent $w(x)$ of the highly stressed region is a finite, thickness independent fraction of the width W , while the length scales with L_t , as seen upon rescaling with $\bar{x} \equiv x\tau^{1/2}/W$. We therefore identify this as a *diffuse-stress* region.

This observation is not inconsistent with the previously noted stress-focusing apparent near $x \approx L_t$, as the diffuse-stress region terminates at $\bar{x}^* \approx 0.32$, beyond which a focused-stress structure appears. This structure resembles a d cone whose features become sharper as $t \rightarrow 0$, consistently with known scaling laws [9,17]. In contrast to the diverging size WL_t of the diffuse-stressed region, the focused-stress structure is confined to an area $\sim W^2$.

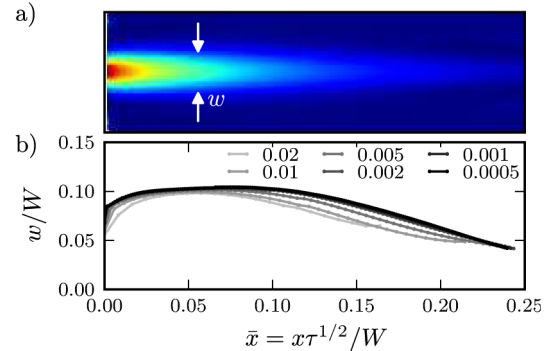


FIG. 2 (color online). (a) The density of stretching energy in the diffuse-stress region of Fig. 1(b). The prescribed edge is at the left. The energy density is well approximated as $A(x) \times \exp[-(y/w(x))^2]$. (b) When plotted against $\bar{x} = x\tau^{1/2}/W$, the width $w(\bar{x})$ is independent of thickness (t/W as indicated).

Our results demonstrate the emergence of a focused-stress domain in response to smooth strainless confinement, and its coexistence with a large diffuse-stress region. Evidence for the general occurrence of such shapes can be obtained by allowing the planar edge profile to rotate an arbitrary angle θ around the y axis [$u_x(x=0, y) = A_3 \cos\theta \cos(3\pi y/W)$]. While this freedom does slightly modify the shape, we found no qualitative change unless the edge was allowed to assume a nonplanar shape [i.e., an arbitrary $u_x(x=0, y)$]. In this case, shown in Fig. 1(c), only a focused-stress structure appears near the edge, giving way to the single buckle after a distance $L_f \sim W$. This length does not depend on thickness, reflecting the geometrical nature of the inextensibility constraint [25]. The energy associated with this focused-stress structure is observed to scale with $\tau^{8/3}$ [26], similar to the energy scaling of minimal ridges [2,10]. This energy is asymptotically negligible relative to the diffuse-stress energy, (3). The “fine-tuning” required to eliminate the diffuse-stress region suggests that although stress focusing is energetically favorable, it is generally insufficient to relieve the strain in a confined sheet. The diffuse-stress region seems to be the “second best” alternative, and hence we conjecture that a coexistence of these two building blocks, focused-stress and diffuse-stress, is a general feature of very thin sheets under arbitrary confinements.

The coexistence of these two markedly different regions in a single shape raises the expectation that an analytic description requires the matching of two distinct types of asymptotic expansions. The asymptotic nature of focused-stress structures is known to reflect a geometric principle [2]: a piecewise-inextensible shape, with vertices and ridges whose size vanishes as $t \rightarrow 0$. Our next step is then to obtain a second, analogous criterion for diffuse-stress structures.

As seen in the estimation of the energies, the diffuse-stress region is characterized by a diverging aspect ratio: $W/L_f \rightarrow 0$ as $\tau \rightarrow 0$. This feature is associated with a mechanical constraint: a vanishing ratio between compressive and tensile stress components. This is seen most clearly by considering the Airy potential $\chi(x, y)$ [7]. The scaling behavior leading to Eq. (3) suggests that in the limit $\tau \ll 1$ Airy potentials of sheets with various thicknesses satisfy a scaling solution: $\chi(x, y) = \tau \tilde{\Delta} Y W^2 g(\tilde{x}, \frac{y}{W})$. Since g is a function only of the rescaled coordinates, it depends only on the geometry of the system and boundary conditions. The prefactor is chosen to satisfy the scaling relations (3). Because of the different scaling of x and y derivatives, the asymptotic stresses scale as

$$\sigma_{xx} \sim Y \tilde{\Delta} \tau \quad \sigma_{yy} \sim Y \tilde{\Delta} \tau^2 \quad \sigma_{xy} \sim Y \tilde{\Delta} \tau^{3/2}. \quad (4)$$

This asymptotic behavior is confirmed in Fig. 3, and shows that as $\tau \rightarrow 0$ a single stress component σ_{xx} becomes dominant. This is unlike the asymptotic behavior of the strain, where Eqs. (2) and (4) imply

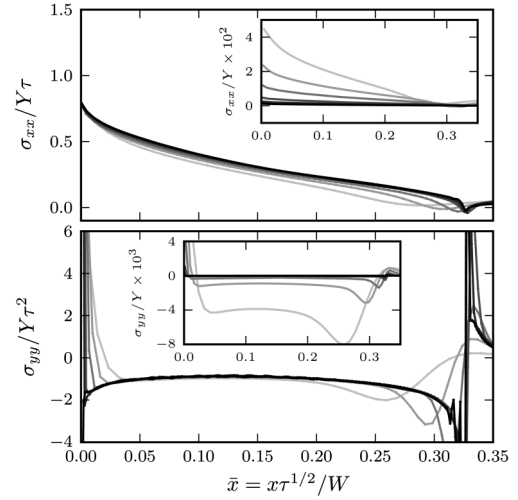


FIG. 3. The diagonal stress components σ_{xx} and σ_{yy} , measured along the centerline of the shapes and plotted against the scaled \bar{x} , for the simulations of Fig. 2(b) (same legend). The data collapse when σ_{xx} is rescaled by τ (top) and σ_{yy} by τ^2 (bottom). Inset: the unscaled stresses, also plotted against \bar{x} .

$$u_{xx} \sim \tilde{\Delta} \tau \quad u_{yy} \sim -\nu \tilde{\Delta} \tau \quad u_{xy} \sim \tilde{\Delta} \tau^{3/2}. \quad (5)$$

This leads us to conjecture that a diffuse-stress region is generally characterized by a vanishing stress ratio:

$$\sigma_{yy}/\sigma_{xx} \rightarrow 0 \quad \text{as} \quad \tau \rightarrow 0, \quad (6)$$

regardless of the Poisson ratio. This mechanical property contrasts with the geometric, piecewise-inextensibility constraint of focused-stress structures. Condition (6) implies that the diffuse-stress region must terminate where the tensile stress σ_{xx} vanishes, as it does for sufficiently large x , in the single buckle region (whereas σ_{yy} remains finite for any τ due to the confinement). This suggests that the focused-stress region appears precisely where condition (6) can no longer be satisfied.

The vanishing stress ratio throughout the whole diffuse-stress region provides a basis for an asymptotic expansion of the shape in the limit $\tau \ll 1$. The simple geometry of our system enables us to demonstrate the basic principle of this expansion, since a natural candidate for the asymptotic diffuse-stress shape is obtained by a decomposition into two leading Fourier modes:

$$\zeta(\bar{x}, y) \approx f_1(\bar{x}) \cos(\pi y/W) + f_3(\bar{x}) \cos(3\pi y/W) \quad (7)$$

for $0 < \bar{x} < \bar{x}^*$, where both functions $f_1(\bar{x})$, $f_3(\bar{x})$ remain finite and higher order modes [e.g., $f_n(\bar{x})$ with $n > 3$] vanish as $\tau \rightarrow 0$. Intuitively, $f_3(\bar{x})$ is finite due to the imposed 3-buckle profile at $x = 0$ whereas $f_1(\bar{x})$ must be finite in the approach to the 1-buckle shape. The ansatz (7) is supported by our numerics, Fig. 4. Obviously, the simple form (7) does not describe the focused-stress region. The FvK equations [7] then provide a nonlinear coupling between the shape $\zeta(\bar{x}, y)$ and the Airy potential $\chi(\bar{x}, y)$,

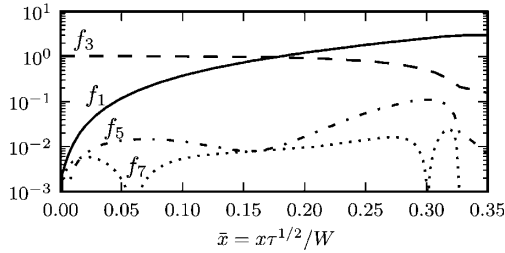


FIG. 4. A linear-log plot of the first four odd Fourier modes of the cross sections of the shapes for $t/W = 0.0005$. Except near the focused structure at $\bar{x}^* \approx 0.32$, modes higher than 3 are negligible, indicating that most of the shape is smooth.

and imply a similar asymptotic expansion for χ that exhibits precisely the vanishing stress ratio (6) [27]. Equation (7) results from the simple geometry of Fig. 1, but we expect that similarly smooth forms, composed of finite number of suitable basis functions, describe the shape and stress distribution of diffuse-stress domains in more complicated geometries. In our case, for $\tau \ll 1$, the FvK equations reduce to a set of coupled ordinary differential equations (ODE) for $f_1(\bar{x})$ and $f_3(\bar{x})$. We expect this reduction to ODE form to be characteristic of diffuse-stress domains. A full solution would require matching of the diffuse-stress shape (7) to the focused-stress structure at \bar{x}^* . The explicit form of the equations, as well as the effective matching conditions, will be discussed elsewhere [26].

We conclude by noting the possible relevance of our results for non-Euclidean elasticity, which addresses the shape of sheets whose strainless state corresponds to some nonflat “target” metric [4,28]. Such sheets are naturally bent even without any external confinement, and are often assumed to be close to an “isometric embedding”, a strainless shape compatible with the target metric. This reasoning is reminiscent of focused-stress regions, wherein the sheet becomes strainless nearly everywhere except in ridges and vertices whose area vanishes asymptotically. However, there may be domains analogous to diffuse-stress zones, where the strain becomes small everywhere in a region of diverging size. Thus, several distinct expansions would need to be stitched together to describe the whole sheet. It remains to be seen whether such a scenario emerges in non-Euclidean sheets.

In summary, we identified two classes of elastic building blocks that can be described as focused-stress and diffuse-stress, and showed how they coexist in elastic sheets under weak, smooth confinement. These two classes are distinguished not only by their stress distributions, but also by their distinct characteristic energies and different underlying asymptotic constraints: a geometric constraint (piecewise inextensibility) for focused-stress domains and a mechanical constraint [Eq. (6)] for diffuse-stress regions. These observations were made by studying an elementary setup that leads to coexistence

between a single focused-stress domain and a single diffuse-stress region that channels stretching along a direction dictated by the uniaxial confinement. Further progress will be required to develop these concepts into a theoretical toolbox for efficient analysis of thin sheets subject to general types of forcing.

We thank B. Audoly, A. Boudaoud, and the authors of [22] for stimulating discussions and for providing us manuscripts of [15,22] before publication. We acknowledge support by NSF-MRSEC on Polymers at UMass (R.S.) and the Petroleum Research Fund of ACS (B.D.). We thank the Aspen Center for Physics for its hospitality.

- [1] J. Genzer and J. Groenewold, *Soft Matter* **2**, 310 (2006).
- [2] T. A. Witten, *Rev. Mod. Phys.* **79**, 643 (2007).
- [3] E. Sharon, M. Marder, and H. Swinney, *Am. Sci.* **92**, 254 (2004).
- [4] J. Dervaux and M. Ben Amar, *Phys. Rev. Lett.* **101**, 068101 (2008).
- [5] N. Bowden *et al.*, *Nature (London)* **393**, 146 (1998).
- [6] J. Huang *et al.*, *Science* **317**, 650 (2007).
- [7] L. Landau and E. Lifshitz, *Theory of Elasticity* (Pergamon, Oxford, 1998).
- [8] M. B. Amar and Y. Pomeau, *Proc. R. Soc. A* **453**, 729 (1997).
- [9] E. Cerda *et al.*, *Nature (London)* **401**, 46 (1999).
- [10] A. E. Lobkovsky, *Phys. Rev. E* **53**, 3750 (1996).
- [11] S. C. Venkataramani, *Nonlinearity* **17**, 301 (2004).
- [12] E. Cerda and L. Mahadevan, *Phys. Rev. Lett.* **90**, 074302 (2003).
- [13] J. Huang *et al.*, *Phys. Rev. Lett.* **105**, 038302 (2010).
- [14] L. Mahadevan, A. Vaziri, and M. Das, *Europhys. Lett.* **77**, 40003 (2007).
- [15] B. Audoly and Y. Pomeau, *Elasticity and Geometry* (Oxford University Press, Oxford, 2010).
- [16] H. Aharoni and E. Sharon, *Nature Mater.* **9**, 993 (2010).
- [17] M. Das *et al.*, *Phys. Rev. Lett.* **98**, 014301 (2007).
- [18] W. Jin and P. Sternberg, *J. Math. Phys. (N.Y.)* **42**, 192 (2001).
- [19] H. Ben Belgacem *et al.*, *J. Nonlinear Sci.* **10**, 661 (2000).
- [20] S. Conti, A. DeSimone, and S. Müller, *Comput. Methods Appl. Mech. Eng.* **194**, 2534 (2005).
- [21] B. Davidovitch, *Phys. Rev. E* **80**, 025202 (2009).
- [22] H. Vandeparre *et al.*, <http://xxx.lanl.gov/abs/1012.4325>.
- [23] K. Brakke, *Exp. Math.* **1**, 141 (1992).
- [24] P. J. de Pablo *et al.*, *Phys. Rev. Lett.* **91**, 098101 (2003).
- [25] A d cone characterized by a diverging length ($L_t \sim t^{-1/3}$) emerges in a pinched cylinder [17]. In contrast to our problem, pointwise pinching introduces a microscopic scale (l) to the geometry, and allows for $t \ll W \ll L_t$.
- [26] R. D. Schroll *et al.* (to be published).
- [27] The corresponding expansion for χ is: $\chi(\bar{x}, \bar{y} \equiv \pi y/W) = \chi_0(\bar{x})\bar{y}^4 + B(\bar{x})\bar{y}^2 + D(\bar{x}) + \sum_{n=1}^3 \chi_{2n}(\bar{x}) \cos 2n\bar{y}$, where the χ_j can be expressed in terms of f_1 and f_3 , and $B(\bar{x})$ and $D(\bar{x})$ are integration constants.
- [28] E. Efrati, E. Sharon, and R. Kupferman, *Phys. Rev. E* **80**, 016602 (2009).